Med Biol Eng Comput (2016) 54:663–674
DOI 10.1007/s11517-015-1357-9

ORIGINAL ARTICLE

Wearable pendant device monitoring using new wavelet-based methods shows daily life and laboratory gaits are different

Matthew A. D. Brodie[1,2] · Milou J. M. Coppens[1] · Stephen R. Lord[1] · Nigel H. Lovell[2] · Yves J. Gschwind[1] · Stephen J. Redmond[2] · Michael Benjamin Del Rosario[2] · Kejia Wang[2] · Daina L. Sturnieks[1] · Michela Persiani[1] · Kim Delbaere[1]

Received: 24 July 2014 / Accepted: 14 July 2015 / Published online: 6 August 2015
© International Federation for Medical and Biological Engineering 2015

Abstract Morbidity and falls are problematic for older people. Wearable devices are increasingly used to monitor daily activities. However, sensors often require rigid attachment to specific locations and shuffling or quiet standing may be confused with walking. Furthermore, it is unclear whether clinical gait assessments are correlated with how older people usually walk during daily life. Wavelet transformations of accelerometer and barometer data from a pendant device worn inside or outside clothing were used to identify walking (excluding shuffling or standing) by 51 older people (83 ± 4 years) during 25 min of 'free-living' activities. Accuracy was validated against annotated video. Training and testing were separated. Activities were only loosely structured including noisy data preceding pendant wearing. An electronic walkway was used for laboratory comparisons. Walking was classified (accuracy ≥97 %) with low false-positive errors (≤1.9 %, $\kappa \geq 0.90$). Median free-living cadence was lower than laboratory-assessed cadence (101 vs. 110 steps/min, $p < 0.001$) but correlated ($r = 0.69$). Free-living step time variability was significantly higher and uncorrelated with laboratory-assessed variability unless detrended. Remote gait impairment monitoring using wearable devices is feasible providing new ways to investigate morbidity and falls risk. Laboratory-assessed gait performances are correlated with free-living walks, but likely reflect the individual's 'best' performance.

Keywords Gait analysis · Wavelet · Remote · Wearable devices · Falls

✉ Matthew A. D. Brodie
brodiephd@gmail.com; matthew.brodie@neura.edu.au

Milou J. M. Coppens
milou.coppens@radboudumc.nl

Stephen J. Redmond
s.redmond@unsw.edu.au

Michael Benjamin Del Rosario
m.delrosario@unsw.edu.au

Kejia Wang
kejia.wang@unsw.edu.au

Daina L. Sturnieks
d.sturnieks@neura.edu.au

Michela Persiani
michela.persiani3@unibo.it

[1] Falls and Balance Research Group, Neuroscience Research Australia, University of New South Wales, Barker Street, Randwick, Sydney, NSW 2031, Australia

[2] Graduate School of Biomedical Engineering, University of New South Wales, Randwick, Sydney, NSW, Australia

1 Introduction

Quantitative gait parameters have been associated with neuromuscular gait disorders [24], fall risk [10], physical activity [32], and the effect of exercise [21]. Laboratory gait assessment mostly uses electronic walkways, passive marker systems, and footswitches in standardized laboratory settings [18]. Laboratory gait assessments have good psychometric properties; however, relationships between straight line reference walks in controlled settings [30] and less constrained walks [1, 14] or walking during daily life [26] require further investigation.

Recent technological developments in wearable sensors have made remote activity monitoring in 'free-living' environments possible [22, 26]. Algorithms have been developed to identify and assess different types of physical activities, for example: peaks associated with steps or strides [12], sit-to-stand transfers [22], and walking on stairs or level ground [25, 29, 35].

However, accuracy of these algorithms to assess activities of daily life may strongly rely on correct device positioning and orientation [13], and elaborate set-up may be required. Previous studies have used waist, leg, ankle, and/or sternum-mounted sensor devices to collect accelerometer and/or barometric pressure data [1, 13, 22, 33, 35]. Compared to structured laboratory studies, reported performance of activity classification algorithms drops in daily life simulations [11], or if the training and validation groups are independent [9]. The detection of less-structured walks during daily life activities is often confused with quiet standing and shuffling movements [1, 9, 11], especially in older people with impaired mobility [13]. Thresholds may either be set for high sensitivity (87–94 % [11]), with correspondingly high false-positive errors (19–28 %), or for low false-positive errors (2 ± 2 % [9]), with correspondingly reduced sensitivity (74 ± 30 %) to detect walking periods.

For classifying activities, wavelet transformations [13] of acceleration data may be better than Fourier transformations [4, 36]. Wavelets provide new ways of investigating gait complexity [29] or abnormalities such as stumbles [15]. Here, we present a new method to remotely monitor gait impairments, which combines discrete wavelet decomposition with decision tree algorithms. Wavelets are good for describing local regularities in gait signals [12] and, for example, already accepted for heart monitoring of ventricular arrhythmias [3]. In this study, the Daubechies 'db5' wavelet is used. The 'db5' wavelet is widely used in signal processing applications due to its simplicity and continuous first-order derivative [2].

In remote and prolonged monitoring applications involving older adults, it may be more difficult to ensure strict compliance and precise device placement. Freely worn devices providing similar accuracy [9, 17] have advantages. Acceptance of pendant devices by independent living people at risk of falls may be inferred from the many Personal Emergency Response Systems (PERS) commercially available, which generally include discrete pendant sensors.

In summary, previous work suggests several limitations with remote gait assessments during unrestricted free-living settings. Issues include: reliance on correct device positioning; confusion between walking, shuffling, and quiet standing; and understanding about how free-living gait relates to laboratory-assessed gait. Therefore, as part of the current study, semi-structured daily activities by 51 older adults were recorded using a freely worn pendant sensor. Our objectives were to investigate: (a) whether a new wavelet-based decision tree algorithm could distinguish continuous walking from shuffling movements with both high sensitivity and low false-positive errors; (b) how walking during daily activities relates to laboratory-assessed gait; and therefore, (c) whether remote gait analysis with a freely worn pendant device is feasible.

2 Methods

2.1 Overview

Fifty-one older people wore a small pedant device and completed 25–30 min of 'free-living' activities (Fig. 1). Annotated video was used as the gold standard. To identify periods of walking, decision tree algorithms were developed based on wavelet transformations of the data. To investigate how walking as part of daily life activities relates laboratory assessment, gait was also measured using an electronic walkway. Algorithm code and example data are available from the author.

2.2 Participants

Fifty-one community-dwelling older adults (83 ± 4 years) were recruited from the fourth wave of the Sydney Memory and Ageing Study [28]. Participants able to walk with or without a walking aid participated in the study. The study was approved by the University of New South Wales Human Studies Ethics Committee, and all participants provided informed consent prior to participation. Age, height, weight, body mass index (BMI), and physiological fall risk assessed using the Physiological Profile Assessment (PPA) [20] were recorded.

2.3 The inertial pendant device and unrestricted placement

Participants wore the Philips® Senior Mobility Monitor (SMM, Philips Research Europe, Eindhoven, Netherlands) on a lanyard around their neck without further restrictions. The pendant (39.5 × 12 × 63.5 mm) contained a triaxial accelerometer and a barometer. The accelerometer had a sampling frequency of 50 Hz and range of ±8 G. The barometer had a sampling frequency of 25 Hz and an operating pressure range of 10–1200 hPa. The pendant's lanyard length was adjusted to a self-selected height and worn inside or outside clothing. Data were stored on an SD card inside the SMM and extracted for processing on a desktop computer after the experiment was complete.

2.4 Free-living walking during semi-structured activities in a semi-controlled environment

The free-living experiment comprised 25–30 min of daily activities [34] that people might perform in their home environment (see Fig. 1). Durations were dependent on the functional performance of each participant. Activities were performed at Neuroscience Research Australia in a semi-controlled environment where corridors often contained other people walking. Free-living activities were

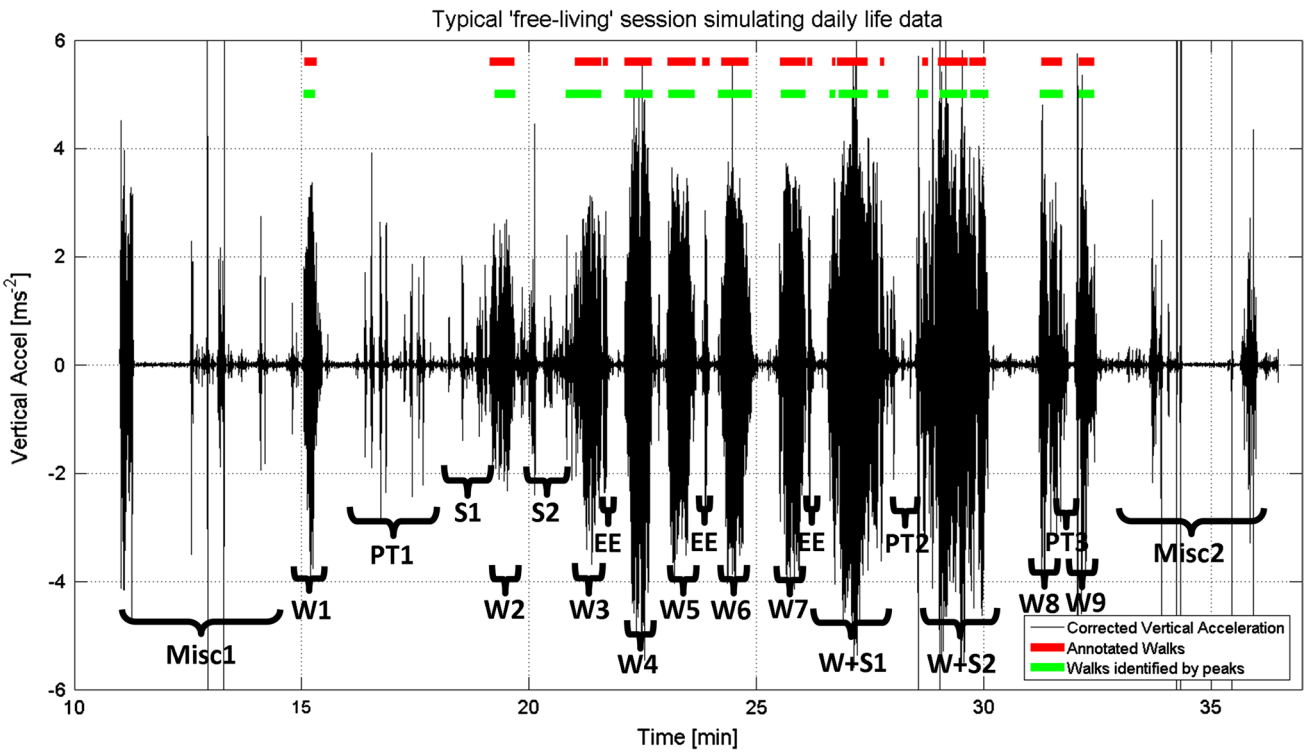

Fig. 1 Example annotated vertical acceleration data from the semi-structured 'free-living' experiment. Key: *W1–W9*—walks of various lengths often bounded by postural transfers. *W+S1* and *W+S2*—walks including stairs. *PT1* to *PT3*—various stand/sit/recline postural transfers. *S1* and *S2*—various 'shuffling' movements and tasks within a room. *Misc1* and *Misc2*—miscellaneous movements associated with setting up the experiment, including synchronization, carrying the device, and putting the device on. *EE*—elevator entry after waiting on the landing. Note: Walks annotated by the video (*top horizontal lines*) and detected by the new wavelet method (*second horizontal lines*) are visualized at the top of the figure. For this 'athletic' participant, the few steps taken when entering the elevator (EE) caused most confusion

semi-structured; participants were asked to perform several tasks in a given order, but were not given specific instructions about how to complete each task.

Tasks included: sitting down on soft and hard chairs, lying down on a sofa, switching power outlets at floor level, and light switches at shoulder level. In one of the tasks, participants were asked to go to a kitchen bench, pour themselves a cup of water, carry the cup to a table, pull a chair out, sit down, drink from the cup, return to the kitchen bench, and wash their cup in a sink. Other tasks included bending to put rubbish in the bin, walking through corridors, walking between rooms, moving about within a room, taking the elevator, walking up and down stairs, and stopping to look out windows.

2.5 Video annotation

For validation, free-living activities were simultaneously recorded with a hand-held video camera. Activities were annotated by a trained observer, using custom software to record the precise timings. Annotated 'walking' required continuous stepping, progression down a corridor or between spaces, and was defined between the first and last heel strikes. Continuous stepping required at least three consecutive heel strikes that had to be no more than 3 s apart. Shuffling movements within a room were annotated as 'not walking'; for example, moving a short distance from sink to table. Stair negotiation was separated from continuous walking for decision trees one (DT1) and two (DT2), but not for decision tree three (DT3); see Tables 1 and 2.

2.6 Wavelet interpretations of free-living activities

For the wavelet detection of continuous walking over flat ground, participants were randomly assigned to independent training ($n = 25$) and testing groups ($n = 26$). In addition to the unrestricted device placement, further mechanisms were devised to simulate 'worst-case' remote monitoring scenarios. For 3 min before the participant put on the inertial pendant (approximately 10 % of the active duration, see Fig. 1, Misc1), the device was exposed to unrestricted movements: randomly picked up, carried about the room, swung by the lanyard, passed from person to

Table 1 Grid search specifications and global optimum values for three different decision tree algorithms using the training group ($n = 25$)

Threshold variable	Start	Step	Stop	Chosen value		
				DT1	DT2	DT3
Max transition accel (m/s^2)	1.8	0.2	3	2.2	2.4	2.6
Max pressure change (Pa/s)	1.5	0.5	4	2.5	3	NA
Min step peak (m/s^2)	0.3	0.1	1	0.5	0.5	0.5
Min steps (count)	4	2	18	10	10	16
Frequency ratio	1	0.25	2.5	NA	1.75	1.75

Table 2 Classification performance for the testing group ($n = 26$) by three different decision tree algorithms using the thresholds determined in the training group ($n = 25$)

	DT1	DT2	DT3
Number of nodes	4	5	4
Stair climbing separated	Yes	Yes	No
Kappa	0.90	0.91	0.93
Accuracy (%)	97.1	97.3	97.9
False-positive errors (%)	1.6	1.6	1.3
Sensitivity to walking (%)	90.9	92.1	94.6

person, and synchronized by hitting it twice against a table top.

Discrete wavelet decomposition was performed using the Daubechies 'db5' wavelet to transform the acceleration signal into an array of coefficients (Fig. 2a), whereby coefficients at each subsequent level (vertical axis) represent signal power at half the previous mid-pseudo-frequency. In Fig. 2a, level 1 represents signal power at the mid-pseudo-frequency of 16 Hz, level 2 at 8 Hz, level 3 at 4 Hz, level 4 at 2 Hz, level 5 at 1 Hz, level 6 at 0.5 Hz, level 7 at 0.25 Hz, and level 8 at 0.13 Hz. As frequency resolution increases, temporal resolution decreases (horizontal axis) and the coefficients at subsequent levels each cover twice the time period. Normalized signal strength is plotted (Fig. 2a) from zero (black) to one (white). This provides an efficient way to simultaneously identify both frequency and temporal changes associated with steps taken during continuous walking.

Inspection of the training set revealed several pertinent features, which in combination showed potential to identify continuous walking. Postural transitions causing changes in device orientation, such as the recline-to-stand (Fig. 2d), were characterized by detail levels 6 and 7 of the triaxial acceleration (vertical only shown), corresponding to mid-pseudo-frequencies of approximately 0.25 and 0.5 Hz, respectively. The direction of a transition (Fig. 2e), such as the sit-to-stand (upwards) or stair negotiation, was characterized by pressure changes in the level 6 approximation of the differentiated barometer signal, which were negatively correlated with height changes. Rhythmical heel strikes while walking (Fig. 2c) were characterized by peaks in detail levels 4 and 5 of the vertical acceleration (corresponding to mid-pseudo-frequencies of approximately 1 and 2 Hz) and could be separated from similar peaks during miscellaneous impacts by the frequency ratio. Vertical acceleration (Fig. 2b) was extracted, using a level 7 approximation of the gravity vector to correct for low-frequency changes in device orientation, similar to previous methods [5]. The frequency ratio was calculated over consecutive 62 point (≈1.2 s) moving average data windows by dividing the level 4 and 5 details of vertical acceleration by the level 1 and 2 details of vertical acceleration. Window length for frequency ratio was selected to encompass at least two heel strikes at an expected step frequency of 1.6 Hz.

2.7 Wavelet detection of continuous walking using decision trees

Three empirical decision tree algorithms were developed to identify continuous walking. The first decision tree (DT1, Fig. 3) had four nodes and was designed to separate continuous walking from all other activities including stair climbing. The first two decision nodes rejected data where orientation changes or height changes were above thresholds expected during walking over flat ground (Figs. 2d, e). The third node retained data containing heel strike peaks above a set threshold (Fig. 2c, circles). Finally, the fourth node only retained walks with more than a set number of consecutive heel strike peaks (Fig. 2c, horizontal band).

The second decision tree (DT2) had five decision nodes, additionally using the frequency ratio. In this case, a walk also required stepping frequencies (details 4 and 5) to be significantly greater than higher frequencies (details 1 and 2) associated with some miscellaneous movements.

The third decision tree (DT3) did not use the barometer data and therefore had only four decision nodes. Consequently, in this case no attempt was made to separate stair climbing from walking.

2.8 Grid search and classification performance

Agreement between continuous walking detected by the algorithms and walking annotated in the recorded videos

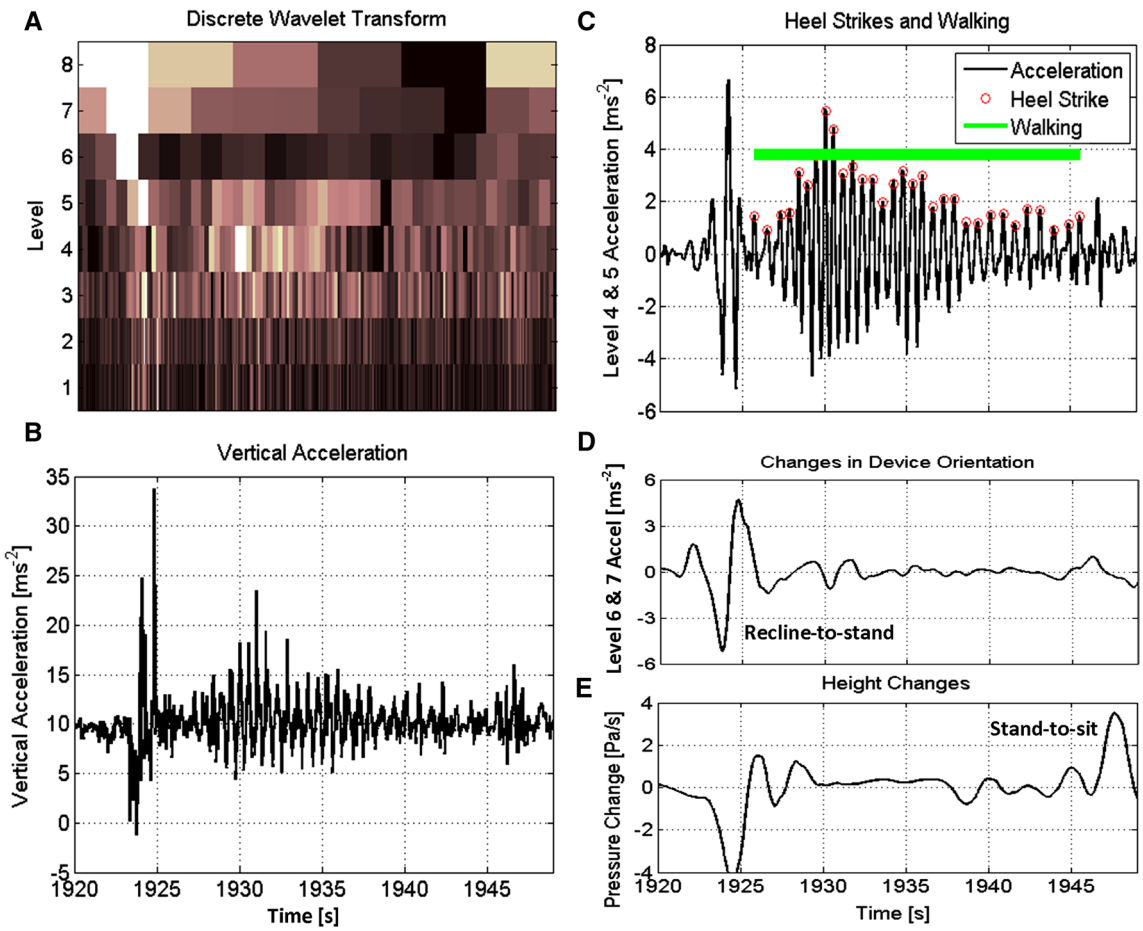

Fig. 2 Wavelet-based analysis of free walk W9 (Fig. 1). **a** Wavelet decomposition of the active period using Daubechies 'db5' wavelet. Level 1 (mid-pseudo-frequency 16 Hz) to level 8 (mid-pseudo-frequency 0.13 Hz) on the *vertical axis*. Time is on the *horizontal axis* and identical to **b** underneath. Normalized signal strength is visualized from zero (*black*) to one (*white*). **b** Corrected vertical acceleration. **c** Heel strikes identified by peaks greater than 0.5 m/s^2 in the level 4 and 5 (mid-pseudo-frequencies 1 and 2 Hz) wavelet details (*circles*), and a walk by 10 or more consecutive steps (*thick line*). **d** Postural transitions excluded by changes in device orientation greater than 2.2 m/s^2 in the level 6 and 7 (0.5 and 0.25 Hz) wavelet details. **e** Postural transitions excluded by pressure changes greater than 2.5 Pa/s, which are negatively correlated with height. Note: This participant wore the pendant swinging freely over clothing, and no orientation changes were observed during the stand-to-sit transition, but the height change was picked up by the barometer

was calculated using Cohen's Kappa because it accounts for sample bias [16] and incorporates all elements of the confusion matrix. A Kappa of unity indicates perfect agreement. Grid searches (Table 1) were performed in MATLAB® 2013a using data from the 25 participants in the training group. Threshold values (Table 2) residing in the geometric centre of a broad plateau representing global optimum performance (Fig. 3, left panel) were selected. Performance was then validated using data from the 26 participants of the testing group (Table 2). We also calculated accuracy (defined as the percentage of all activities correctly classified) false-positive errors (defined as the percentage of incorrectly identified walks) and sensitivity (defined as the percentage of correctly identified walks).

2.9 Clinical assessment

Participants were instructed to perform three walks at their usual walking speed on a 4.60 m GaitRite® electronic walkway (CIR Systems Inc. Clifton, NJ 07012). All walks were performed according to the European guidelines for clinical applications of spatiotemporal gait analysis in older adults [19]. Gait parameters were obtained from GaitRite® software version 3.3 and included speed (cm/s), cadence

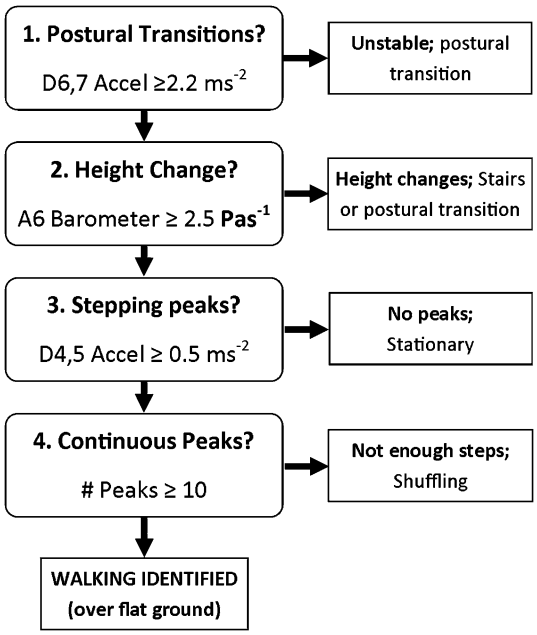

Fig. 3 A decision tree algorithm (DT1) for identifying continuous walking over flat ground. Walking required at least 10 steps (node 4) with no large changes in height (node 2) or device orientation (node 1). More nodes could be added to identify other activities of daily life

(steps/min), step length (cm), and the standard deviation (SD) of step times (s).

2.10 Wavelet assessment of free-living walking

2.10.1 Cadence

A peak detection algorithm was used to identify steps in walks previously classified by the first wavelet detection algorithm (DT1, Fig. 3). Peaks in the detail levels 4 and 5 of the vertical acceleration were counted, provided they were greater than half the threshold selected in the previous grid search and were between 300 and 3000 ms apart. Free-living cadence was then calculated as the number of peaks counted divided by walk duration in minutes. From all free-living walks greater than 10 steps (the threshold for DT1) by each participant, the 2.5, 25, 50, 75, and 97.5 cadence percentiles were recorded.

2.10.2 Step time variability and detrended variability

Variability during free-living walks was calculated by the standard deviation of step times in seconds. Step times were calculated by the duration between the successive acceleration peaks previously used to calculate cadence. Detrended variability (Fig. 5) was calculated by subtracting a five-point moving average from the step times prior to obtaining a standard deviation. Detrended variability was calculated to prevent the longer-term changes in cadence, associated with accelerations and decelerations during free-living walks, potentially swamping the shorter-term step time variability. Median values from multiple walks by each participant were recorded.

2.11 Free-living correlates for walking speed and step length

The root-mean-squared (RMS) vertical acceleration [23] and the RMS vertical velocity oscillation were calculated for each walk previously identified by the first wavelet detection algorithm (DT1, Table 1). Vertical velocity oscillations were calculated by integrating vertical acceleration and high-pass filtering using bidirectional fourth-order Butterworth filter with 0.75 Hz cut-off frequency [5]. Median values from multiple walks by each participant were recorded.

2.12 Statistical comparison of free-living walking and laboratory gait assessment

Assumptions for parametric statistic were met. Pearson's correlations and paired t tests were used to investigate possible associations and differences between spatiotemporal gait parameters from free-living and laboratory gait assessments. SPSS 20.0 (SPSS, Inc., Chicago, IL) was used for data analyses with a significance level of 0.05.

3 Results

Participants ranged in age from 76 to 96 (mean 83 ± 4 years), had varied heights (167 ± 9 cm), and had varied weights (69 ± 14 kg). According to their Physiological Profile Assessments, they also had varied physiological fall risk [20] with scores ranging from −0.62 to 2.53 (0.90 ± 0.82). Thirty-one participants were male and twenty were female. Participants were towards the upper healthy range for body mass index (25 ± 3 kg/m^2).

3.1 Wavelet-based decision tree detection of continuous walking

During the semi-structured daily activities, we observed orientation and position of the device relative to the subjects' thorax could change. Device movement could be unpredictable, as the device could become temporally entangled in clothing or participants could 'fiddle' with the device. Despite this noisy data, the training grid search revealed a robust solution space, with strong agreement between walks detected by the algorithm and the video annotation. Within a broad peak of optimum Kappa (Fig. 4,

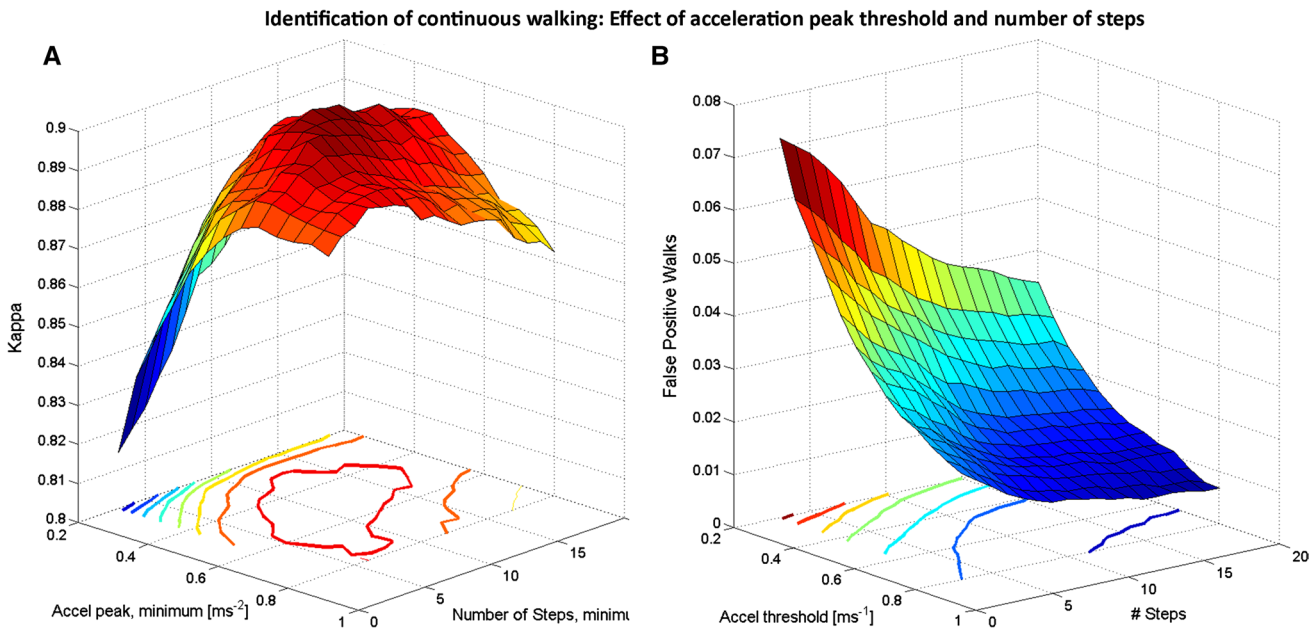

Fig. 4 Effects of minimum acceleration peak threshold and number of steps in the identification of continuous walking for Cohen's Kappa (**a**) and false-positive errors (**b**). **a** Shows that optimum classification of continuous walking forms a broad peak approximately centred around thresholds of 0.5 ms^{-2} and 10 steps. **b** Shows that increasing both the peak acceleration for step detection and the number of steps required for continuous walking reduces the false-positive errors or the amount of shuffling and quiet standing mistaken for walking

left panel), algorithm performance plateaued and was relatively insensitive to small changes in thresholds. Final thresholds for the first decision tree (Table 1) required continuous walking to have at least 10 consecutive steps with acceleration peaks greater than 0.5 m/s^2. Postural transitions and/or stair climbing were excluded by thresholds of 2.2 m/s^2 and 2.5 Pa/s (equating to a rate of height change of around 18 cm/s).

In the test group, the thresholds for the first decision tree (DT1) resulted in good agreement with the annotated video (κ 0.90, accuracy 97.1 %, sensitivity 90.9 %, and low false-positive errors of 1.6 %, Table 2). For the second decision tree, increasing decision tree complexity by adding a node for the frequency ratio ($\geq$1.75) slightly improved performance (κ 0.91). The third decision tree, which did not use barometer data, also had marginally better performance (κ 0.93), but could not separate stair climbing from walking.

3.2 Associations between free-living and laboratory gait analysis

Compared to the laboratory assessment of cadence on the electronic walkway (110 ± 9 steps/min, Table 3), participants had significantly lower median cadence during free-living (101 ± 7 steps/min, $p < 0.001$), but no significant difference was observed for maximum free-living cadence ($p < 0.19$). Furthermore, maximum free-living cadence was most correlated with laboratory-assessed cadence ($r = 0.80$, $p < 0.001$). Laboratory assessment of step length was most correlated with RMS vertical velocity oscillation during free-living ($r = 0.71$, $p < 0.001$). Laboratory assessment of walking speed was most correlated with RMS vertical acceleration during free-living ($r = 0.68$, $p < 0.001$).

Compared to laboratory assessment of step time variability (19 ± 10 ms, Table 3) from constant speed walking, participants had significantly higher step time variability in the free-living environment (103 ± 53 ms, $p < 0.001$). A significant correlation was observed between laboratory assessment of step time variability and detrended step time variability in the free-living environment ($r = 0.31$, $p < 0.03$).

4 Discussion

4.1 Wavelet-based decision tree detection of continuous walking

Accurate identification of continuous walking during activities of daily life was feasible using the freely worn inertial pendant sensor (κ 0.90, accuracy 97 %). Different to previous research, our main focus was on the problematic distinction between continuous walking, shuffling, and quiet standing. This singular focus enabled both high

Table 3 Spatiotemporal gait parameters assessed by accelerometer and compared to an electronic walkway

Gait parameter	Laboratory	Free-living	Correlated	Paired *t* test
	Mean ± SD		Pearson's r (*p*)	*p*-value
Cadence [steps/min]	109.9 ± 8.5			
Median [peaks/min]		100.9 ± 7.4	0.69 (<0.001)	<0.001
UQ [peaks/min]		104.8 ± 7.9	0.76 (<0.001)	<0.001
Max [peaks/min]		108.9 ± 7.9	0.80 (<0.001)	0.19
Step length (cm)	60.9 ± 9.8			
RMS VT Velocity [cm/s]		11.2 ± 2.9	0.71 (<0.001)	<0.001
Velocity (cm/s)	111 ± 20			
RMS VT Accel [m/s^2]		1.54 ± 0.34	0.68 (<0.001)	<0.001
Step time variability [ms]	19 ± 10			
variability [ms]		103 ± 53	0.27 (0.06)	<0.001
Detrended variability [ms]		82 ± 46	0.31 (0.03)	<0.001

sensitivity (90.9 %) and low false-positive errors (1.6 %) to be obtained. Previously, during free-living simulations, high sensitivity has been achieved using a device fixed to the lower back [11], and low false-positive errors have been achieved using a mobile phone [9], but not simultaneously.

One strength of the new wavelet-based decision tree algorithms was that despite several mechanisms devised to simulate 'worst-case' real-world scenarios we still observed low false-positive errors. For example, the device was fiddled with, carried in the hands of a technician, randomly lifted up, and banged down on a table. Furthermore, including data from a barometer enabled stair climbing to be separated from walking.

Similar to others [25], our approach defined continuous walking by consecutive heel strikes. However, in the current study the device was worn freely and not rigidly strapped to a bony landmark. Compared to more structured experiments [22], for example involving a fixed ten metre walk [12], we did not achieve 100 % accuracy. The difference may relate to our semi-structured experimental design and noise from miscellaneous activities, which were included to reduce the likelihood of overtraining. Our older participants (76–96 years of age) were of varied height, weight, and physical capacity. They completed many walks of varied lengths including shuffling and various activities while quite standing (Fig. 1). Variability in the training data increases the likelihood that similar performance will be obtained during future remote and prolonged monitoring applications.

In our training group, increasing the number of steps required for a walk reduced the false-positive errors (Fig. 4, right panel). However, because our participants completed both short and long walks, increasing the number of steps required for a walk also increased the number of walks missed. Therefore, within the 'plateau of optimum performance', increasing the number of steps required for a walk resulted in little change to overall performance (Fig. 4, left panel). The annotated videos revealed that most errors were due to confusion between shuffling and walking. Walks were missed (causing decreased sensitivity) if too few steps were taken, for example, by the more athletic participants taking 'too few' longer steps to enter the elevator (see Fig. 1, EE). Conversely, false-positive errors were caused by prolonged shuffling, which the video annotator deemed to be without the purpose of getting to a new location, for example, by the more 'frail' participants taking 'too many' shorter steps while moving to the sink.

Improved performance was achieved by increasing algorithm complexity (κ 0.91), and by not excluding stair climbing from the definition of continuous walking (κ 0.93). Personalizing the thresholds may have led to further improvements. However, these alternative solutions were not used in our final solution (DT1) because we considered the marginal improvements did not justify the increased risk of overtraining and in the second part of the experiment, data from flat walking without any stair climbing were required. A decision tree approach may trade performance for increased interpretability and reduced complexity [7]. Our final solution successfully identified free-living

Fig. 5 Step times during free-living walks varied both in the shorter term (*thin line*) and in the longer term (*thick line*) as participants slowed down to avoid obstacles. During free-living, detrended variability was calculated by subtracting the moving average (*thick line*) from the step times (*thin line*) prior to obtaining the standard deviation. Detrended variability was correlated with the laboratory assessment of step time variability

walking patterns using just four decision nodes that had direct physical interpretations. With respect to the 'big data' requirements of population monitoring, a decision tree approach may provide computational efficiencies because at each node only a subset of the computations is required. For example, during long-term monitoring, if some 'inactive' periods of data were rejected by the top level node processing time would be reduced, because full computations would not be required for all data.

During selection of global thresholds, a robust moving average approach was used to avoid being 'caught' by any local maxima. In the training group, we observed a 'plateau of optimum performance' (Fig. 4, left panel) with many local maxima likely reflecting the finite limitations of the data set and discontinuities associated with step counting. Algorithm thresholds were therefore selected from the estimated geometric centre of this 'plateau', which was our best estimate of the global optimum solution.

We acknowledge certain limitations. One issue with using discrete wavelet transforms is shift variance [27, 31], whereby the wavelet coefficients may depend on the distance from the start of the data window to the signal of interest. Because the expected step frequency during continuous walking was around 1.6 Hz, any changes caused by shift invariance would be likely to inversely affect the level 4 coefficients (mid-pseudo-frequency 2 Hz) relative to the level 5 coefficients (mid-pseudo-frequency 1 Hz). Error associated with shift invariance was therefore minimized by combining the level 4 and 5 details and using the inverse discrete wavelet transform prior to heel strike detection. Furthermore, test–retest reliability of the method was not assessed. However, in a subsequent study the long-term measurement stability of the new method has been established using 8 weeks of remote monitoring [6].

4.2 Associations between free-living and laboratory gait analysis

We found significant correlations between laboratory gait analysis and free-living walking for measures of maximum cadence ($r = 0.80$, $p < 0.001$), step length ($r = 0.71$, $p < 0.001$), walking speed ($r = 0.68$, $p < 0.001$), and detrended step time variability ($r = 0.31$, $p = 0.03$). However, free-living walks had significantly slower median cadences and greater step time variability (both $p < 0.001$), and no significant difference was found for maximum free-living cadence ($p < 0.19$). Together, these observations suggest that laboratory gait measurements do relate to free-living walking, but are more indicative of an individual's 'best' performance, and not their usual performance. Therefore, both laboratory and free-living assessments might potentially provide complementary information about morbidity risk and fall risk.

Older adults tend to reduce their cadence, velocity, and step length with increasing age, and our laboratory gait assessments were within expected margins [18, 30]. Interestingly, step time variability during free-living walking (103 ± 53 ms) was approximately five times greater than when assessed in the laboratory with an electronic walkway (19 ± 10 ms) and not significantly correlated. One explanation could be that in the laboratory setting only steady-state straight walking was recorded, whereas fluctuating cadences were recorded during the free-living walks. We observed that step times often changed over several steps in the free-living walks (Fig. 5). Participants often accelerated at the start of a walk and slowed down as they approached various obstacles. Detrended step time variability was therefore calculated which removed these longer-term cadence changes. Although detrended step time variability was still greater (82 ± 46 s) than laboratory-assessed step time variability, it was significantly correlated ($r = 0.31$, $p = 0.03$).

Differences between free-living and laboratory assessments might also be explained by participants being more aware of measurements being taken during a clinical assessment. Participants might focus more on walking when travelling over an electronic walkway compared to assessment of daily activities when walks are measured using a discrete wearable device.

We observed that more vigorous participants, who walked faster and had greater step lengths during laboratory assessments, also had greater vertical accelerations ($r = 0.68$, $p < 0.001$) and greater vertical velocity oscillations ($r = 0.71$,

$p < 0.001$) during free-living walks. These correlates were chosen because it was not practical to measure walking speed or step lengths directly from the pendant accelerations. However, vertical accelerations are correlated with walking speed squared [23], and principal component analysis has been used to show that many measureable gait features map to few underlying principal components, such as gait intensity or vigour [8], which comprises of step length, walking speed, vertical oscillations, and accelerations.

5 Conclusion

The new wavelet-based decision tree method accurately separated continuous walking from shuffling and other movements during the activities of daily life. Laboratory gait assessments correlated with free-living walking, but likely reflected an individual's 'best' performance. Remote gait impairment monitoring using freely worn devices appears feasible and provides new ways to investigate morbidity and fall risk. Future work might investigate whether remote gait monitoring can be incorporated into existing pendant Personal Emergency Response Systems. The objective assessments of changes in gait quantity and gait quality over time could then be used to alert the associated healthcare providers of deteriorating health and/or increasing fall risk in participants.

Acknowledgments We gratefully acknowledge support which made this research possible. Devices were lent from Philips Research Europe, Netherlands. M.B., S.L., and K.D. were NHMRC Fellows, Australia. Y.G. was supported by the Margarete and Walter Lichtenstein Foundation, Switzerland.

References

1. Aminian K, Robert P, Buchser EE, Rutschmann B, Hayoz D, Depairon M (1999) Physical activity monitoring based on accelerometry: validation and comparison with video observation. Med Biol Eng Comput 37(3):304–308
2. Ayrulu-Erdem B, Barshan B (2011) Leg motion classification with artificial neural networks using wavelet-based features of gyroscope signals. Sensors (Basel, Switzerland) 11(2):1721–1743. doi:10.3390/s110201721
3. Balasundaram K, Masse S, Nair K, Umapathy K (2013) A classification scheme for ventricular arrhythmias using wavelets analysis. Med Biol Eng Comput 51(1–2):153–164. doi:10.1007/s11517-012-0980-y
4. Barralon P, Vuillerme N, Noury N (2006) Walk detection with a kinematic sensor: frequency and wavelet comparison. Conf Proc Ann Int Conf IEEE Eng Med Biol Soc IEEE Eng Med Biol Soc Conf 1:1711–1714. doi:10.1109/iembs.2006.260770
5. Brodie MA, Beijer TR, Canning CG, Lord SR (2015) Head and pelvis stride-to-stride oscillations in gait: validation and interpretation of measurements from wearable accelerometers. Physiol Meas 36(5):857–872. doi:10.1088/0967-3334/36/5/857
6. Brodie MA, Lord SR, Coopens MJ, Annegarn J, Delbaere K (2015) Eight weeks of remote monitoring using a freely worn device reveals unstable gait patterns in older fallers. Aheadofprint, IEEE Trans Bio-med Eng. doi:10.1109/TBME.2015.2433935
7. Brodie MA, Lovell NH, Redmond SJ, Lord SR (2015) Bottom-up subspace clustering suggests a paradigm shift to prevent fall injuries. Med Hypotheses 84(4):356–362. doi:10.1016/j.mehy.2015.01.017
8. Brodie MA, Menz HB, Lord SR (2014) Age-associated changes in head jerk while walking reveal altered dynamic stability in older people. Exp Brain Res 232(1):51–60. doi:10.1007/s00221-013-3719-6
9. Del Rosario MB, Wang K, Wang J, Liu Y, Brodie M, Delbaere K, Lovell NH, Lord SR, Redmond SJ (2014) A comparison of activity classification in younger and older cohorts using a smartphone. Physiol Meas 35(11):2269
10. Delbaere K, Sherrington C, Lord SR (2013) Chapter 70—falls prevention interventions. In: Marcus R, Feldman D, Dempster DW, Luckey M, Cauley JA (eds) Osteoporosis (4th edn). Academic Press, San Diego, pp 1649–1666. doi:10.1016/B978-0-12-415853-5.00070-4
11. Dijkstra B, Kamsma Y, Zijlstra W (2010) Detection of gait and postures using a miniaturised triaxial accelerometer-based system: accuracy in community-dwelling older adults. Age Ageing 39(2):259–262. doi:10.1093/ageing/afp249
12. Godfrey A, Bourke AK, Olaighin GM, van de Ven P, Nelson J (2011) Activity classification using a single chest mounted tri-axial accelerometer. Med Eng Phys 33(9):1127–1135. doi:10.1016/j.medengphy.2011.05.002
13. Godfrey A, Conway R, Meagher D, OL G (2008) Direct measurement of human movement by accelerometry. Med Eng Phys 30(10):1364–1386. doi:10.1016/j.medengphy.2008.09.005
14. Haggard P, Cockburn J, Cock J, Fordham C, Wade D (2000) Interference between gait and cognitive tasks in a rehabilitating neurological population. J Neurol Neurosurg Psychiatry 69(4):479–486
15. Karel JM, Senden R, Janssen JE, Savelberg HM, Grimm B, Heyligers IC, Peeters R, Meijer K (2010) Towards unobtrusive in vivo monitoring of patients prone to falling. Conf Proc Ann Int Conf IEEE Eng Med Biol Soc IEEE Eng Med Biol Soc Conf 2010:5018–5021. doi:10.1109/iembs.2010.5626232
16. Kaymak U, Ben-David A, Potharst R (2012) The AUK: a simple alternative to the AUC. Eng Appl Artif Intell. doi:10.1016/j.engappai.2012.02.012
17. Khan AM, Lee YK, Lee S, Kim TS (2010) Accelerometer's position independent physical activity recognition system for long-term activity monitoring in the elderly. Med Biol Eng Comput 48(12):1271–1279. doi:10.1007/s11517-010-0701-3
18. Kirtley C (2006) Clinical gait analysis. Elsevier, London
19. Kressig RW, Beauchet O (2006) Guidelines for clinical applications of spatio-temporal gait analysis in older adults. Aging Clin Exp Res 18(2):174–176
20. Lord SR, Menz HB, Tiedemann A (2003) A physiological profile approach to falls risk assessment and prevention. Phys Ther 83(3):237–252
21. Mannini A et al (2011) Healthcare and accelerometry: applications for activity monitoring, recognition, and functional assessment. In: Lai DTH, Palaniswami M, Begg R (eds) Healthcare sensor networks: challenges toward practical implementation. CRC Press, New York, pp 21–46
22. Mathie MJ, Celler BG, Lovell NH, Coster AC (2004) Classification of basic daily movements using a triaxial accelerometer. Med Biol Eng Comput 42(5):679–687

23. Moe-Nilssen R (1998) A new method for evaluating motor control in gait under real-life environmental conditions. Part 2: gait analysis. Clin Biomech 13(4–5):328–335
24. Montero-Odasso M, Verghese J, Beauchet O, Hausdorff JM (2012) Gait and cognition: a complementary approach to understanding brain function and the risk of falling. J Am Geriatr Soc 60(11):2127–2136. doi:10.1111/j.1532-5415.2012.04209.x
25. Najafi B, Aminian K, Paraschiv-Ionescu A, Loew F, Bula CJ, Robert P (2003) Ambulatory system for human motion analysis using a kinematic sensor: monitoring of daily physical activity in the elderly. IEEE Trans Bio Med Eng 50(6):711–723. doi:10.1109/TBME.2003.812189
26. Rispens SM, van Schooten KS, Pijnappels M, Daffertshofer A, Beek PJ, van Dieen JH (2015) Identification of fall risk predictors in daily life measurements: gait characteristics' reliability and association with self-reported fall history. Neurorehabilitation Neural Repair 29(1):54–61. doi:10.1177/1545968314532031
27. Runyi Y (2012) Shift-variance analysis of generalized sampling processes. IEEE Trans Signal Process 60(6):2840–2850. doi:10.1109/tsp.2012.2190062
28. Sachdev PS, Brodaty H, Reppermund S, Kochan NA, Trollor JN, Draper B, Slavin MJ, Crawford J, Kang K, Broe GA, Mather KA, Lux O, Memory, Ageing Study T (2010) The Sydney memory and ageing study (MAS): methodology and baseline medical and neuropsychiatric characteristics of an elderly epidemiological non-demented cohort of Australians aged 70–90 years. Int Psychogeriatr 22(8):1248–1264. doi:10.1017/S1041610210001067
29. Sekine M, Tamura T, Akay M, Fujimoto T, Togawa T, Fukui Y (2002) Discrimination of walking patterns using wavelet-based fractal analysis. IEEE Trans Neural Syst Rehabil Eng Publ IEEE Eng Med Biol Soc 10(3):188–196. doi:10.1109/tnsre.2002.802879
30. Senden R, Grimm B, Heyligers IC, Savelberg HH, Meijer K (2009) Acceleration-based gait test for healthy subjects: reliability and reference data. Gait Posture 30(2):192–196. doi:10.1016/j.gaitpost.2009.04.008
31. Serbes G, Aydin N (2014) Denoising performance of modified dual-tree complex wavelet transform for processing quadrature embolic Doppler signals. Med Biol Eng Comput 52(1):29–43. doi:10.1007/s11517-013-1114-x
32. Sims J (2012) Advancing physical activity in older Australians: missed opportunities? Australas J Ageing 31(4):206–207. doi:10.1111/ajag.12002
33. Tolkiehn M, Atallah L, Lo B, Yang GZ (2011) Direction sensitive fall detection using a triaxial accelerometer and a barometric pressure sensor. Conf Proc Ann Int Conf IEEE Eng Med Biol Soc IEEE Eng Med Biol Soc Conf 2011:369–372. doi:10.1109/IEMBS.2011.6090120
34. Wang K, Lovell NH, Del Rosario MB, Ying L, Jingjing W, Narayanan MR, Brodie MAD, Delbaere K, Menant J, Lord SR, Redmond SJ (2014) Inertial measurements of free-living activities: assessing mobility to predict falls. In: Engineering in medicine and biology society (EMBC), 36th annual international conference of the IEEE, 26–30 Aug 2014, pp 6892–6895. doi:10.1109/embc.2014.6945212
35. Yang S, Laudanski A, Li Q (2012) Inertial sensors in estimating walking speed and inclination: an evaluation of sensor error models. Med Biol Eng Comput 50(4):383–393. doi:10.1007/s11517-012-0887-7
36. Zijlstra W, Aminian K (2007) Mobility assessment in older people: new possibilities and challenges. Eur J Ageing 4(1):3–12. doi:10.1007/s10433-007-0041-9

Matthew A. D. Brodie is a NHMRC EC Fellow, Senior Research Officer at Neuroscience Research Australia, Lecturer at UNSW, and 2008 MacDiarmid Young Scientist of the Year (Future Technology Winner).

Milou J. M. Coppens received her M.Sc. degree in Humen Movement Sciences from the University of Groningen in 2014. She is currently a Ph.D. candidate at the Radboudumc Nijmegen.

Stephen R. Lord is a Senior Principal Research Fellow at Neuroscience Research Australia. He has a DSc from UNSW and publishes in the areas of instability, falls, and fractures in older people.

Nigel H. Lovell is currently a Professor at the Graduate School of Biomedical Engineering, UNSW. He is a Fellow of five learned societies throughout the world (FATSE, FIEAust, FIEEE, FIP, and FAIMBE).

Yves J. Gschwind is a visiting postdoctoral research fellow from University Hospital Basel and University of Basel, Switzerland.

Stephen J. Redmond is an ARC Future Fellow at UNSW Sydney. He earned his BE and PhD in 2002 and 2006, respectively, from University College Dublin, Ireland.

Michael Benjamin Del Rosario is a Ph.D. candidate at UNSW. He completed his Bachelor of Engineering (Mechatronic) and Master's Degree in Biomedical Engineering in 2012.

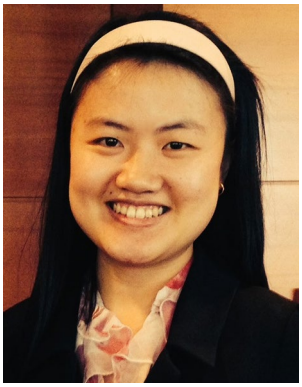

Kejia Wang is a PhD candidate at the Graduate School of Biomedical Engineering, UNSW, Australia. She gained a BE (Hons 1st Class), from the University of Auckland in 2012.

Daina L. Sturnieks has a Ph.D. in biomechanics from the University of Western Australia. She is Senior Research Officer and Laboratory Manager at Neuroscience Research Australia.

Michela Persiani earned a Ph.D. degree in Pharmacology and Toxicology, Human Development and Movement Sciences from the University of Bologna in 2015.

Kim Delbaere is a NHMRC CD Fellow and Group Leader at Neuroscience Research Australia. She uses physiology, psychology, brain imaging, and technology to predict and prevent falls in older people.